J. Iron Steel Res. Int. (2018) 25:146–156
https://doi.org/10.1007/s42243-018-0015-5

ORIGINAL PAPER

Modeling reoxidation behavior of Al–Ti-containing steels by $CaO–Al_2O_3–MgO–SiO_2$ slag

Ying Ren[1] · Li-feng Zhang[1] · Ying Zhang[1]

Received: 30 October 2017 / Revised: 30 October 2017 / Accepted: 31 October 2017 / Published online: 6 February 2018

Abstract
A kinetic model was developed using FactSage Macro Processing to simulate the reoxidation of Al–Ti-containing steels by $CaO–Al_2O_3–SiO_2–MgO$ slags. The calculated results show a good agreement with the experimental data. Thus, the developed kinetic model can be used to predict changes in slag, steel, and inclusion compositions during the reaction process. During the slag reoxidation process, the reactions occurring at slag–steel interface and in the bulk steel were confirmed to be the reduction of SiO_2 by [Al] and [Ti] and the self-dissociation of SiO_2 into [Si] and [O]. Increasing the ratio of CaO to SiO_2 in the slag can significantly suppress the self-dissociation of SiO_2 in the slag and lower the amount of inclusions produced during reoxidation. The formed inclusions changed from solid Al_2O_3 to $Al_2O_3–TiO_x$ inclusions, which was mainly dependent on the w([Al]) and w([Ti]). The amount of inclusions was obviously influenced by the composition of the top slag.

Keywords Kinetic model · Slag · Inclusion · Reoxidation · Al–Ti-containing steel

1 Introduction

As the demand for high-performance steels increases year by year, reoxidation is always one of the challenging issues to improve steel cleanliness [1, 2]. During the refining process of interstitial-free (IF) steels, Al is added for deoxidation. Ti addition is beneficial to bind the elements of C and N by precipitating titanium carbide and nitride during solidification and cooling process [3]. During the ladle standing and tundish casting process, Al and Ti, in particular, are susceptible to oxidation by the air absorption or reducible oxides such as FeO, MnO, and SiO_2 in the slag, fluxes, or refractories [4–8]. As a consequence, there are unwanted Al_2O_3, TiO_x, and Al–Ti–O inclusions formed, resulting in process problems such as nozzle clogging, surface defects, diminishing the effect binding of Ti [9–16].

It is well known that the SiO_2-rich flow guiding sand was added to guarantee smooth continuous casting process, which may give rise to strong reoxidation of the Al–Ti-containing steels [17–19]. Until now, there are few investigations focusing on the combined oxidation of Al and Ti in the steel by SiO_2-rich slag. Park et al. [4] experimentally and thermodynamically investigated reoxidation of the liquid steel containing Al and Ti by 14% CaO–35% Al_2O_3–10% MgO–41% SiO_2 slag at 1823 K. The initial Al in the steel was fixed to be 0.0820 mass%, and Ti content was varied from 0.0100 to 0.0500 mass%. It was proposed that self-dissociation of SiO_2 into [Si] and [O] at the slag–metal interface played an important role in the slag reoxidation process. However, there may be various reoxidation behavior of Al–Ti-containing steels with different w([Al]), w([Ti]), and slag compositions. Thus, it is necessary to investigate the reoxidation behavior of Al–Ti-containing steels in different conditions.

Recently, several kinetic models were developed by using the combination of thermodynamic calculations with simplified fluid dynamic equations of the liquid melt in the ladle. The variation of inclusion, steel, and slag during the ladle treatment process was successfully predicted [20–27]. Furthermore, with the application of thermodynamic software, the optimized thermodynamic data as functions of temperature and composition in a multicomponent system are beneficial to improve the accuracy of kinetic modeling [28]. In the current study, a kinetic model was developed using FactSage Macro Processing to better understand

✉ Li-feng Zhang
zhanglifeng@ustb.edu.cn

[1] School of Metallurgical and Ecological Engineering, University of Science and Technology Beijing, Beijing 100083, China

the reoxidation behavior of Al–Ti-containing steels by CaO–Al_2O_3–MgO–SiO_2 slags.

2 Kinetic model

There are many reactions involved during the slag reoxidation process, as shown in Fig. 1. During the slag reoxidation process, both steel and slag mass transfers are considered to be the possible rate-determining steps. In each time step Δt, the masses of slag and steel transported to the interface mainly depend on the density ρ of phase i, the mass transfer coefficient m_i, and the area of the interface A [24]. Thus, the masses of slag and steel equal to $m_i A \rho_i \Delta t$ are transferred to react to equilibrium for each time step. The slag mass transfer coefficient is expected to be ten times smaller than the mass transfer coefficient in the steel [29]. After the reactions at the interface, the reacted slag and steel were transferred back and mixed with the bulk volumes.

To simplify the model and calculation, the following assumptions are made in the current thermodynamic model: (1) All inclusions in the bulk steel and the bulk slag itself were assumed to be homogeneous in the composition; (2) slag–steel reaction at interface and steel–inclusion reaction were assumed to reach the equilibrium [27]; (3) the temperature can be maintained at a fixed temperature; (4) all oxide inclusions in the steel at interface were assumed to be removed as slag; (5) the floatation rate of inclusions was assumed to be a constant; and (6) the refractory–slag reaction and refractory–steel reaction were neglected in the current model.

In the FactSage software, the Equilib program can be called by the embedded coding called "Macro Processing". All the input conditions and output can be stored and passed to the different equilibrium calculations or externally to a simple text file or Microsoft Excel™ worksheets using this macro processing code [23]. A small program can be written using this macro processing code to achieve the calculations of the reaction steps one by one in the order of reaction number as shown in Fig. 1. The thermodynamic phase equilibrium of all reactions was calculated adiabatically using FactSage with FactPS, FToxid, and FTmisc databases [28].

3 Validation of kinetic model

To verify the accuracy of the developed model, experimental data by Park et al. [4] were referenced and compared with the calculated results. In their study, 10 g of 14% CaO–35% Al_2O_3–10% MgO–41% SiO_2 slag and 30 g of 0.082% Al_t–0.032% Ti_t–0.0016% TO (total oxygen)–0.0010% Si–Fe

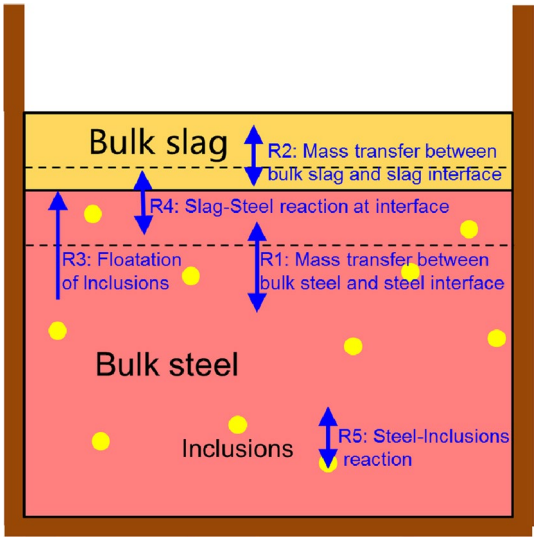

Fig. 1 Schematic diagram of slag–steel–inclusions reactions during slag reoxidation process

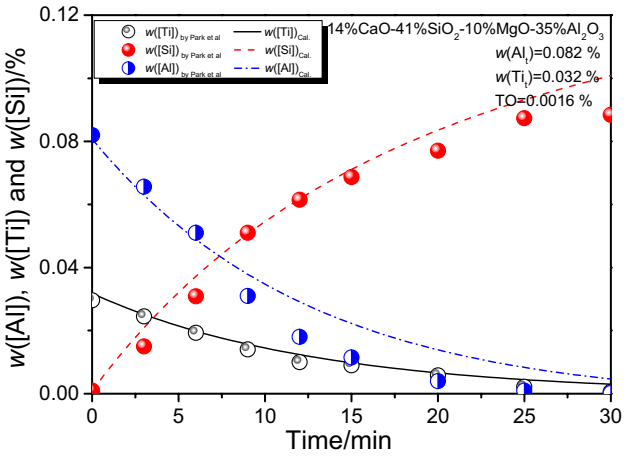

Fig. 2 Measured w([Al]), w([Ti]), and w([Si]) in Al–Ti-containing steels from laboratory experiments [4], compared with modeled behavior for $m_{steel} = 1.0 \times 10^{-5}$ m/s

steel were melted in an alumina crucible (25 mm in inner diameter and 60 mm in height) at 1823 K. Thus, the area of the interface was 0.00049 m^2. The densities of the steel and the slag used in the current calculation were 7000 and 2500 kg/m^3, respectively. The steel mass transfer coefficient of the kinetic model was estimated by fitting experimentally measured concentrations of [Al], [Ti], and [Si]. As shown in Fig. 2, the predicted results show a good agreement with the observed ones, indicating that 1.0×10^{-5} m^3/s is a suitable value of the m_{steel} in the current model.

The TO in the molten steel contains the dissolved oxygen and the oxygen in inclusions. During the reoxidation process, the dissolved oxygen and the inclusion chemistry

were expected to equilibrate with the [Al], [Ti], and [Si]. Meanwhile, the oxygen in inclusions was significantly influenced by the floatation rate of inclusions. Since the predicted and the measured w([Al]), w([Ti]), and w([Si]) were roughly the same, it can be inferred that the floatation rate of inclusions can be estimated by fitting experimentally measured TO in the steel. As can be seen from Fig. 3, with the floatation rate (f) of 0%/s, the calculated TO shows a linear increase, which is obviously higher than the measured results after 20 min. With the floatation rate of 0.1%/s, the calculated TO is obviously lower than the measured ones. The simulated TO with the floatation rate of 0.05%/s shows a similar tendency with the measured TO. Therefore, the floatation rate of inclusions equals 0.05%/s in the current model.

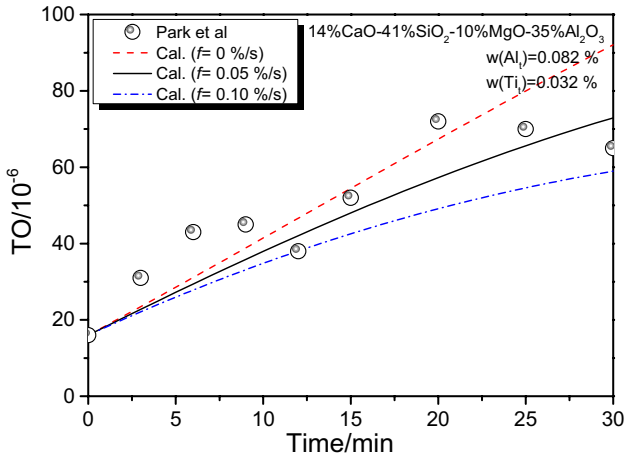

Fig. 3 Measured TO in Al–Ti-containing steels from laboratory experiments [4], compared with modeled behavior with various floatation rates of inclusions

4 Modeling reoxidation behavior of Al–Ti-containing steels with various Al_t, Ti_t, and slag chemistries

To predict the reoxidation behavior of Al–Ti-containing steels with various $w(Al_t)$, $w(Ti_t)$, and slag chemistries, a large number of calculations were apace carried out using FactSage Macro Processing. The masses of the initial steel and slag were 30 and 10 g, respectively. The compositions of the initial steel and slag in the current calculation are listed in Table 1. The temperature in calculation was set as 1823 K.

4.1 Effect of initial Al_t and Ti_t on reoxidation behavior

Figure 4 shows the effect of the initial $w(Al_t)$, $w(Ti_t)$, and slag chemistries on the change of inclusions in Al–Ti-containing steels with 14% CaO–35% Al_2O_3–10% MgO–41% SiO_2 slag. The possible reactions of the inclusion formation are given in Eqs. (1)–(6).

$$2[\mathrm{Al}] + 3[\mathrm{O}] = \left(\mathrm{Al_2O_3}\right)_{\mathrm{inc.}} \tag{1}$$

$$x[\mathrm{Al}] + y[\mathrm{Ti}] + z[\mathrm{O}] = \left(\mathrm{Al}_x\mathrm{Ti}_y\mathrm{O}_z\right)_{\mathrm{inc.}} \tag{2}$$

$$[\mathrm{Ti}] + x[\mathrm{O}] = \left(\mathrm{TiO}_x\right)_{\mathrm{inc.}} \tag{3}$$

$$y[\mathrm{Ti}] + (z - 3x/2)[\mathrm{O}] + x/2\left(\mathrm{Al_2O_3}\right)_{\mathrm{inc.}} = \left(\mathrm{Al}_x\mathrm{Ti}_y\mathrm{O}_z\right)_{\mathrm{inc.}} \tag{4}$$

$$y[\mathrm{Ti}] + z/3\left(\mathrm{Al_2O_3}\right)_{\mathrm{inc.}} = \left(\mathrm{Al}_x\mathrm{Ti}_y\mathrm{O}_z\right)_{\mathrm{inc.}} + (2z/3 - x)[\mathrm{Al}] \tag{5}$$

Table 1 Compositions of initial steel and slag in calculation (%)

No.	Steel				Slag			
	Al_t	Ti_t	TO	Fe	CaO	SiO_2	MgO	Al_2O_3
1	0.01	0.07	0.0016	Balance	14	41	10	35
2	0.02	0.07	0.0016	Balance	14	41	10	35
3	0.03	0.07	0.0016	Balance	14	41	10	35
4	0.04	0.07	0.0016	Balance	14	41	10	35
5	0.03	0.05	0.0016	Balance	14	41	10	35
6	0.03	0.06	0.0016	Balance	14	41	10	35
7	0.03	0.08	0.0016	Balance	14	41	10	35
8	0.03	0.07	0.0016	Balance	9	41	10	40
9	0.03	0.07	0.0016	Balance	19	41	10	30
10	0.03	0.07	0.0016	Balance	10	45	10	35
11	0.03	0.07	0.0016	Balance	20	35	10	35
12	0.03	0.07	0.0016	Balance	30	25	10	35

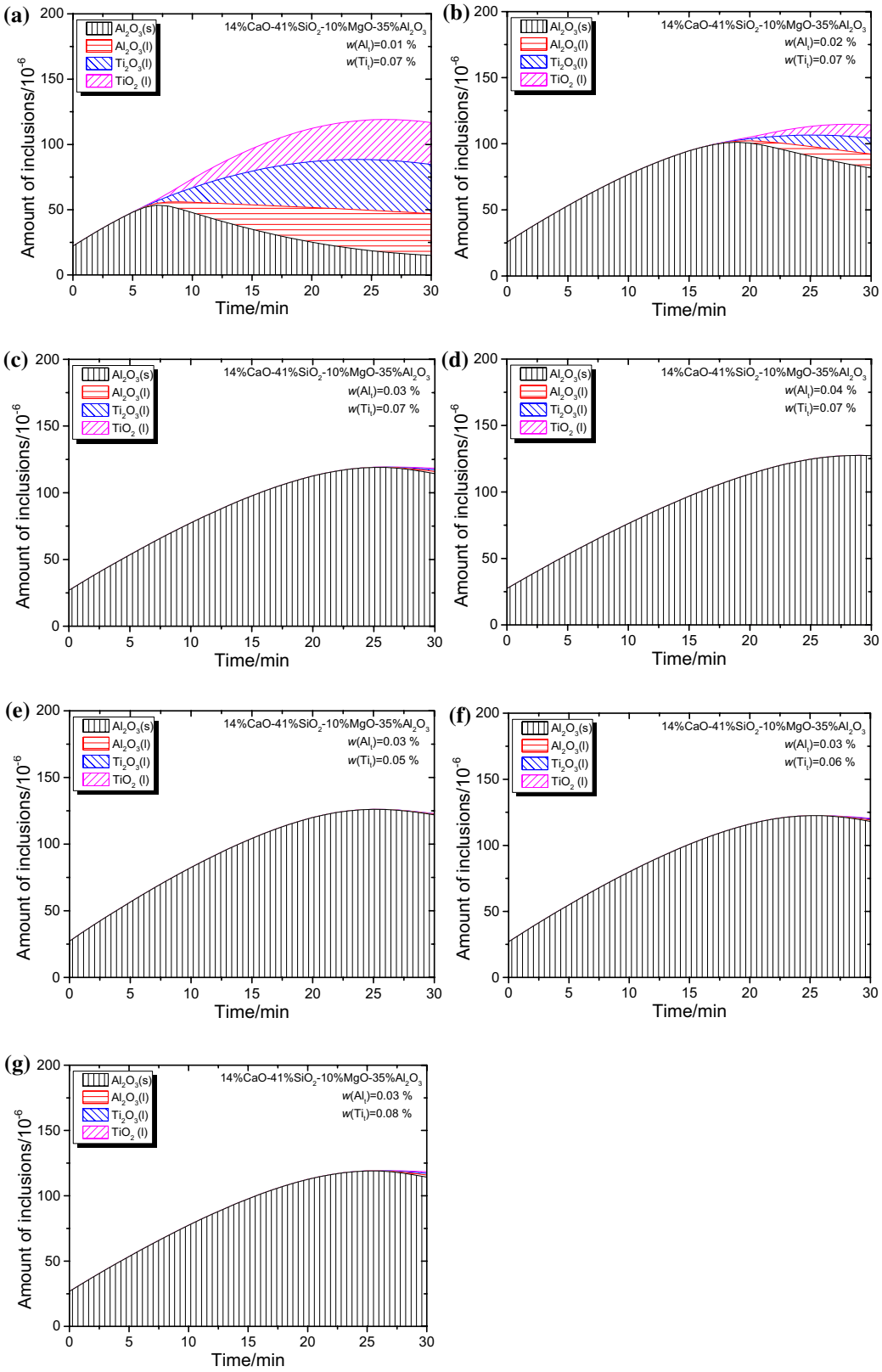

Fig. 4 Effect of initial $w(Al_t)$ and $w(Ti_t)$ on changes of inclusions in Al–Ti-containing steels with 14% CaO–35% Al_2O_3–10% MgO–41% SiO_2 slags

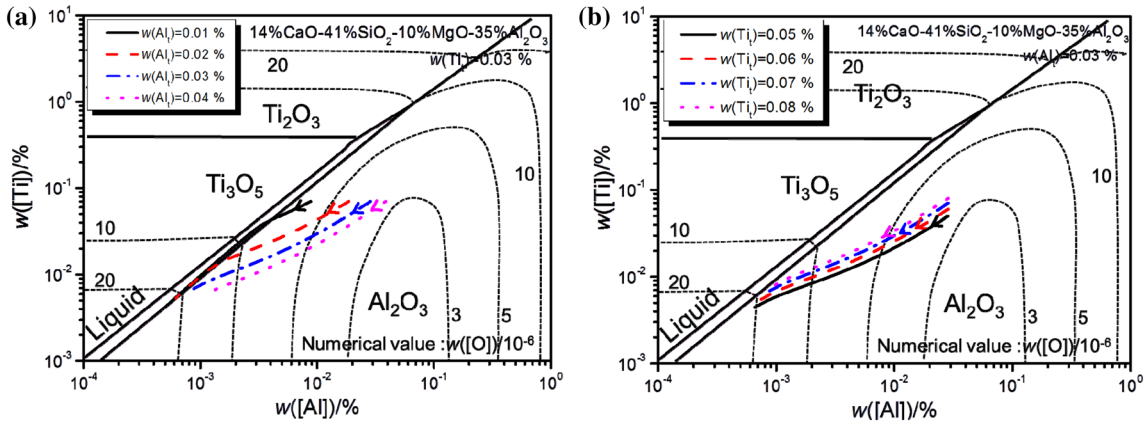

Fig. 5 Effect of initial $w(Al_t)$ and $w(Ti_t)$ on changes in $w([Al])$ and $w([Ti])$ in Al–Ti-containing steels with 14% CaO–35% Al_2O_3–10% MgO–41% SiO_2 slags

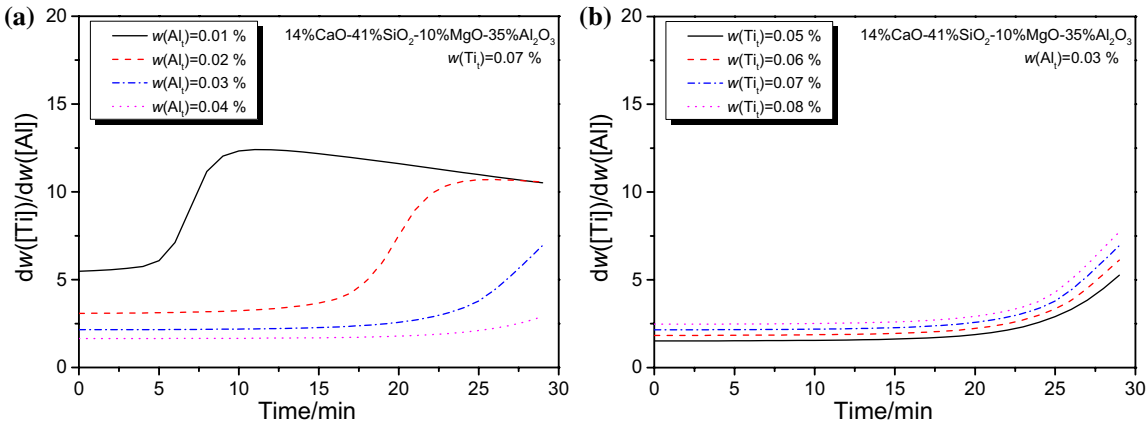

Fig. 6 Effect of initial $w(Al_t)$ and $w(Ti_t)$ on change in $dw([Ti])/dw([Al])$ in Al–Ti-containing steels with 14% CaO–35% Al_2O_3–10% MgO–41% SiO_2 slags

$$3[\mathrm{Ti}] + x\left(\mathrm{Al_2O_3}\right)_{\mathrm{inc.}} = 3\left(\mathrm{TiO}_x\right)_{\mathrm{inc.}} + 2x[\mathrm{Al}] \tag{6}$$

In Fig. 4a–d, the $w(Ti_t)$ was fixed to be 0.07%. In the steel containing 0.01% Al_t, the pure solid Al_2O_3 formed at first, indicating that the formation reaction of Al_2O_3 inclusions in Eq. (1) can occur. Seven minutes later, a large amount of Al_2O_3–TiO_x liquid inclusions were produced. The possible reactions of the formation of Al_2O_3–TiO_x inclusions are given in Eqs. (2) and (3). There was a decline in solid Al_2O_3 inclusions, which was quantified to be caused by the floatation of the inclusions. Thus, it was inferred that the reactions between [Ti] and Al_2O_3 inclusions in Eqs. (4) and (5) can hardly occur during the slag reoxidation process. With the increase in $w(Al_t)$ from 0.01 to 0.04%, the formed Al_2O_3–TiO_x liquid inclusions gradually reduced or disappeared. With the comparison of Fig. 4c, e–f, the formed inclusions in the steel with 0.03% Al_t can hardly be influenced by increasing $w(Ti_t)$ from 0.05 to 0.08%, indicating that the formed inclusion chemistry was mainly dependent on the $w(Al_t)$ and $w(Ti_t)$. Besides, the total amount of the formed inclusions was roughly invariable with the CaO–35% Al_2O_3–10% MgO–41% SiO_2 slag.

The stability diagram of Al–Ti–O inclusions at 1823 K was calculated using FactSage with FactPS, FToxid, and FTmisc databases. Figure 5 shows the effect of the initial $w(Al_t)$ and $w(Ti_t)$ on changes in $w([Al])$ and $w([Ti])$ in Al–Ti-containing steels with the CaO–35% Al_2O_3–10% MgO–41% SiO_2 slag. The direction of the arrows means the changes in $w([Al])$ and $w([Ti])$ with time. It can be seen that the initial $w(Al_t)$ and $w(Ti_t)$ were located in the stability zone of Al_2O_3. With the reoxidation of steels, the $w([Al])$ and $w([Ti])$ moved to the Al_2O_3–TiO_x liquid inclusion zone, agreeing with the observed results shown in Fig. 4. After the steel composition reaching the liquid zone, there were

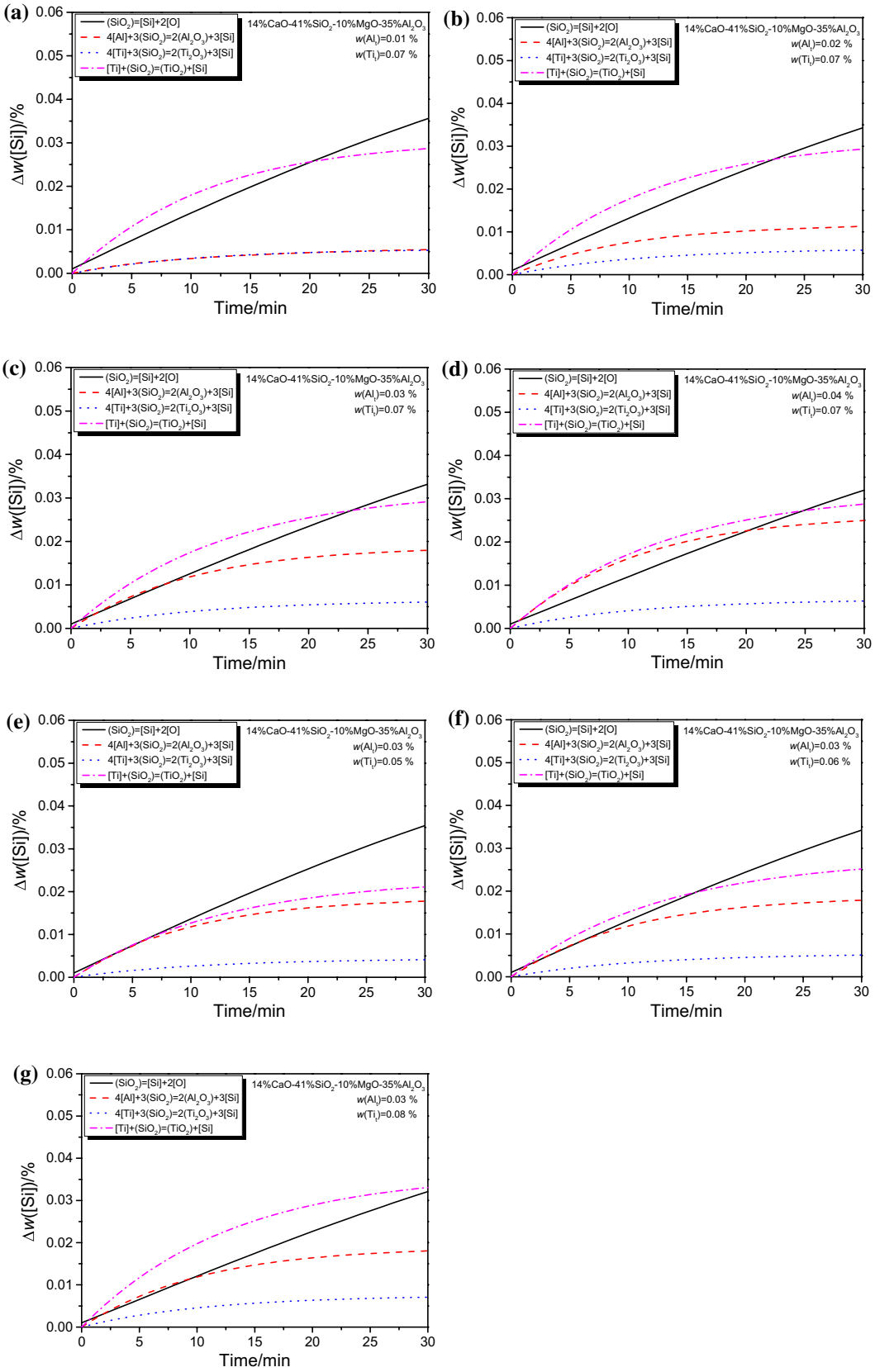

Fig. 7 Effect of initial $w(Al_t)$ and $w(Ti_t)$ on $\Delta w([Si])$ in Al–Ti-containing steels with 14% CaO–35% Al_2O_3–10% MgO–41% SiO_2 slags

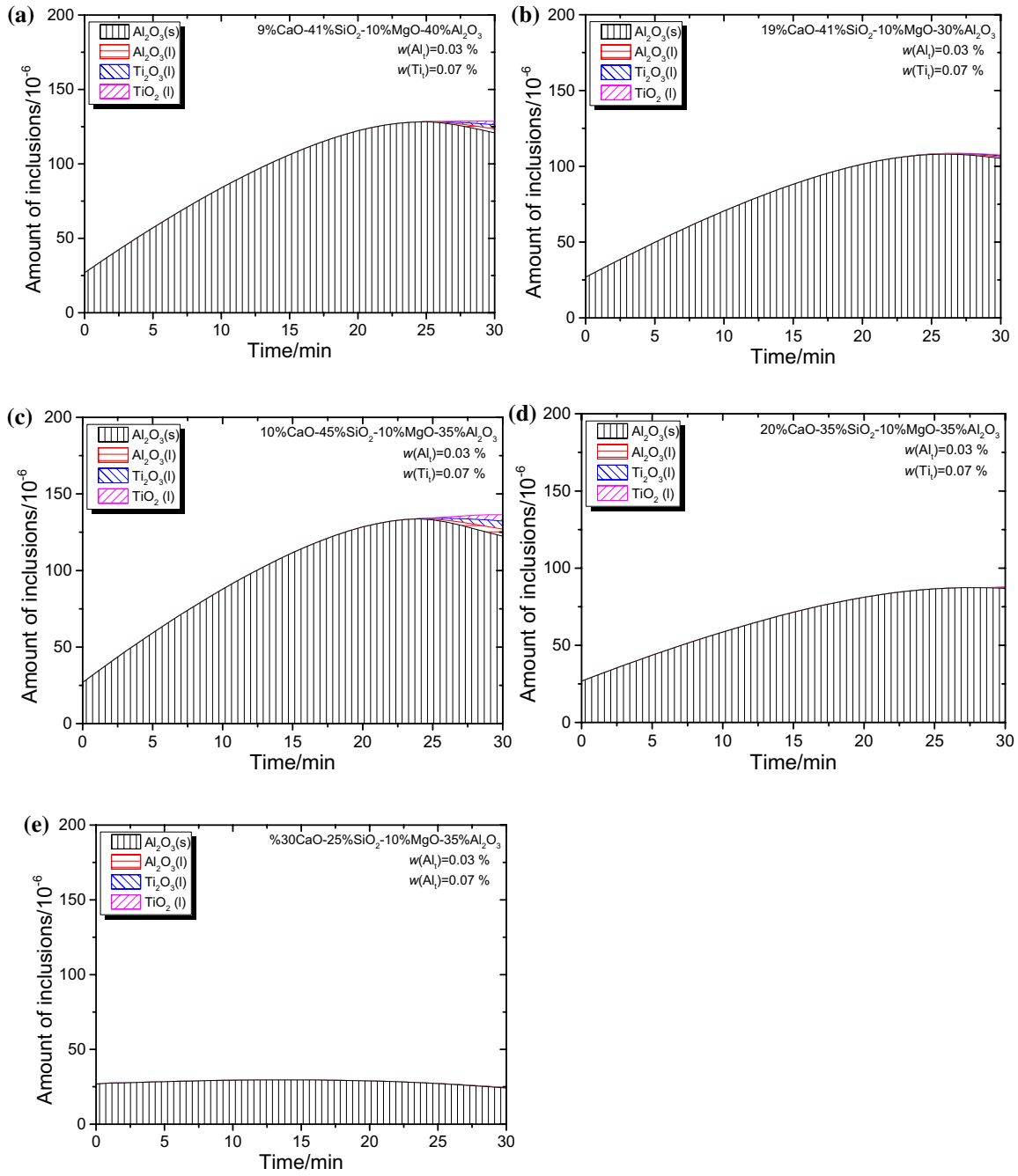

Fig. 8 Effect of initial slag chemistries on changes of inclusions in Al–Ti-containing steels with 0.03% Al_t and 0.07% Ti_t

turning points in the changes in *w*([Al]) and *w*([Ti]). Then, *w*([Al]) and *w*([Ti]) decreased in the liquid zone. Meanwhile, there were no TiO_x inclusions formed in the current calculation, indicating that the reactions in Eqs. (3) and (6) can hardly occur during slag reoxidation. The numerous Al_2O_3–TiO_x liquid inclusions are produced in Fig. 4a owing to the higher ratio of *w*([Ti]) to *w*([Al]) close to the liquid zone.

Figure 6 shows the effect of the initial $w(Al_t)$ and $w(Ti_t)$ on change in d*w*([Ti])/d*w*([Al]) in Al–Ti-containing steels. The d*w*([Ti])/d*w*([Al]) represents the ratio of decrease rate of *w*([Al]) and *w*([Ti]). In Fig. 6a, the d*w*([Ti])/d*w*([Al]) slightly increased at first. The d*w*([Ti])/d*w*([Al]) promptly rose up after [Al] and [Ti] reached the liquid zone as shown in Fig. 5. It indicated that the formation of Al_2O_3–TiO_x liquid inclusion can significantly promote the decrease rate of *w*([Ti]), whereafter the d*w*([Ti])/d*w*([Al]) gradually went

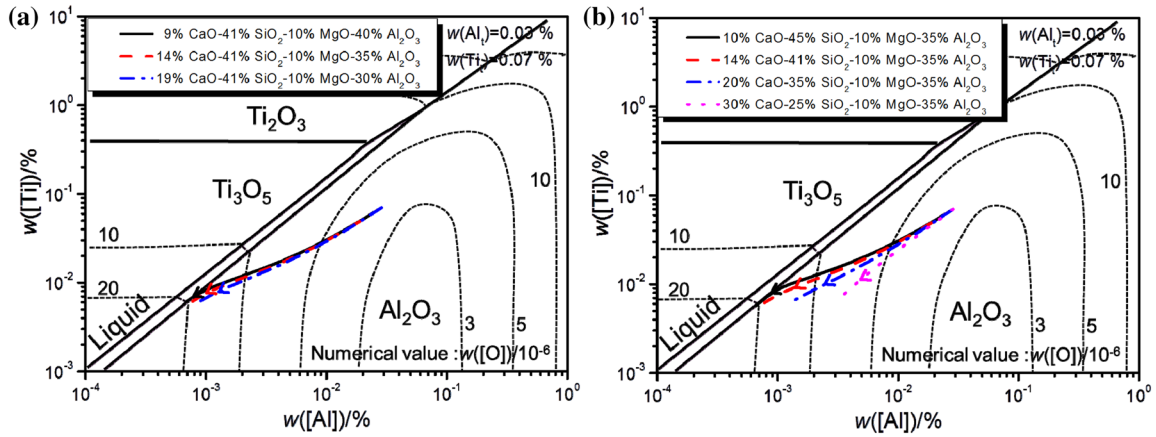

Fig. 9 Effect of initial slag chemistries on changes in [Al] and [Ti] in Al–Ti-containing steels with 0.03% Al_t and 0.07% Ti_t

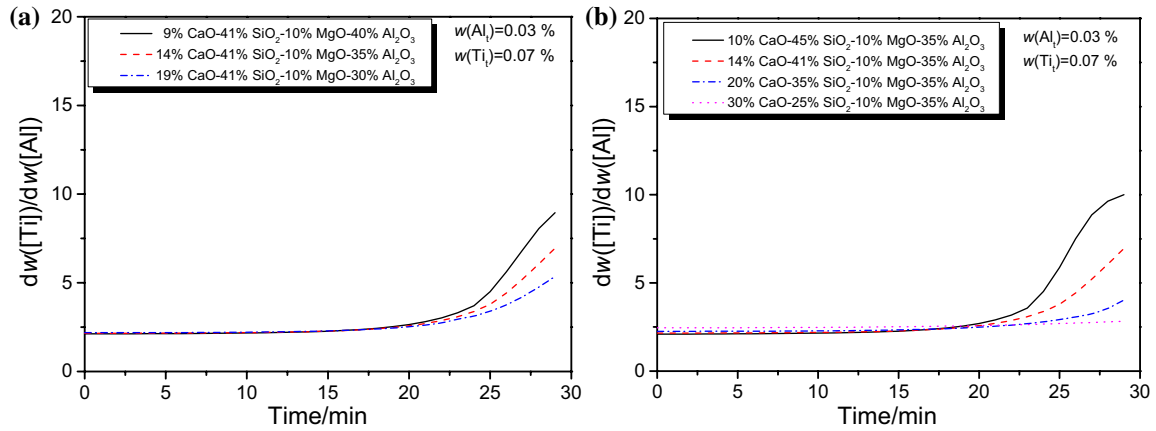

Fig. 10 Effect of initial slag chemistries on change in dw([Ti])/dw([Al]) in Al–Ti-containing steels with 0.03% Al_t and 0.07% Ti_t

down with the evolution of inclusions from pure solid Al_2O_3 to Al_2O_3–TiO_x liquid oxide.

In the current calculation, the oxygen was mainly from the slag. The SiO_2 in the slag was expected to be the only source of oxygen because of its stronger oxidability. During the slag reoxidation process, the w([Si]) gradually went up, which may be caused by the self-dissociation of SiO_2 and the reduction of SiO_2 by Al and Ti. The reactions at the steel–slag interface are given in Eqs. (7)–(10). Since the changes in all formed specifies can be output in the current model, the increase in w([Si]) caused by each reduction reaction can be quantified by the changes in Al_2O_3, Ti_2O_3, and TiO_2 in the slag as Eqs. (8)–(10). Then, the difference in the output [Si] in the steel and the [Si] from the reduction of SiO_2 by [Al] and [Ti] should be caused by the self-dissociation of SiO_2 in Eq. (7). Figure 7 shows the effect of the initial $w(Al_t)$ and $w(Ti_t)$ on Δw([Si]) in Al–Ti-containing steels. The Δw([Si]) means the difference in w([Si]) in the steel caused by each reaction during the slag reoxidation process. It can be seen from Fig. 7a–d that the Δw([Si]) caused by the reduction of SiO_2 in the slag by Al in Eq. (8) significantly goes up with the w([Al]) increasing from 0.01 to 0.04%. Similarly, the Δw([Si]) caused by the reduction of SiO_2 in the slag by Ti in Eqs. (9) and (10) was promoted by the increase in w([Ti]) from 0.04 to 0.08%. However, the Δw([Si]) caused by the self-dissociation of SiO_2 can hardly be influenced by adjusting w([Al]) and w([Ti]) of the steel with the fixed slag composition of 14% CaO–35% Al_2O_3–10% MgO–41% SiO_2.

$$\left(SiO_2\right) = [Si] + 2[O] \tag{7}$$

$$4[Al] + 3\left(SiO_2\right) = 2\left(Al_2O_3\right) + 3[Si] \tag{8}$$

$$4[Ti] + 3\left(SiO_2\right) = 2\left(Ti_2O_3\right) + 3[Si] \tag{9}$$

$$[Ti] + \left(SiO_2\right) = \left(TiO_2\right) + [Si] \tag{10}$$

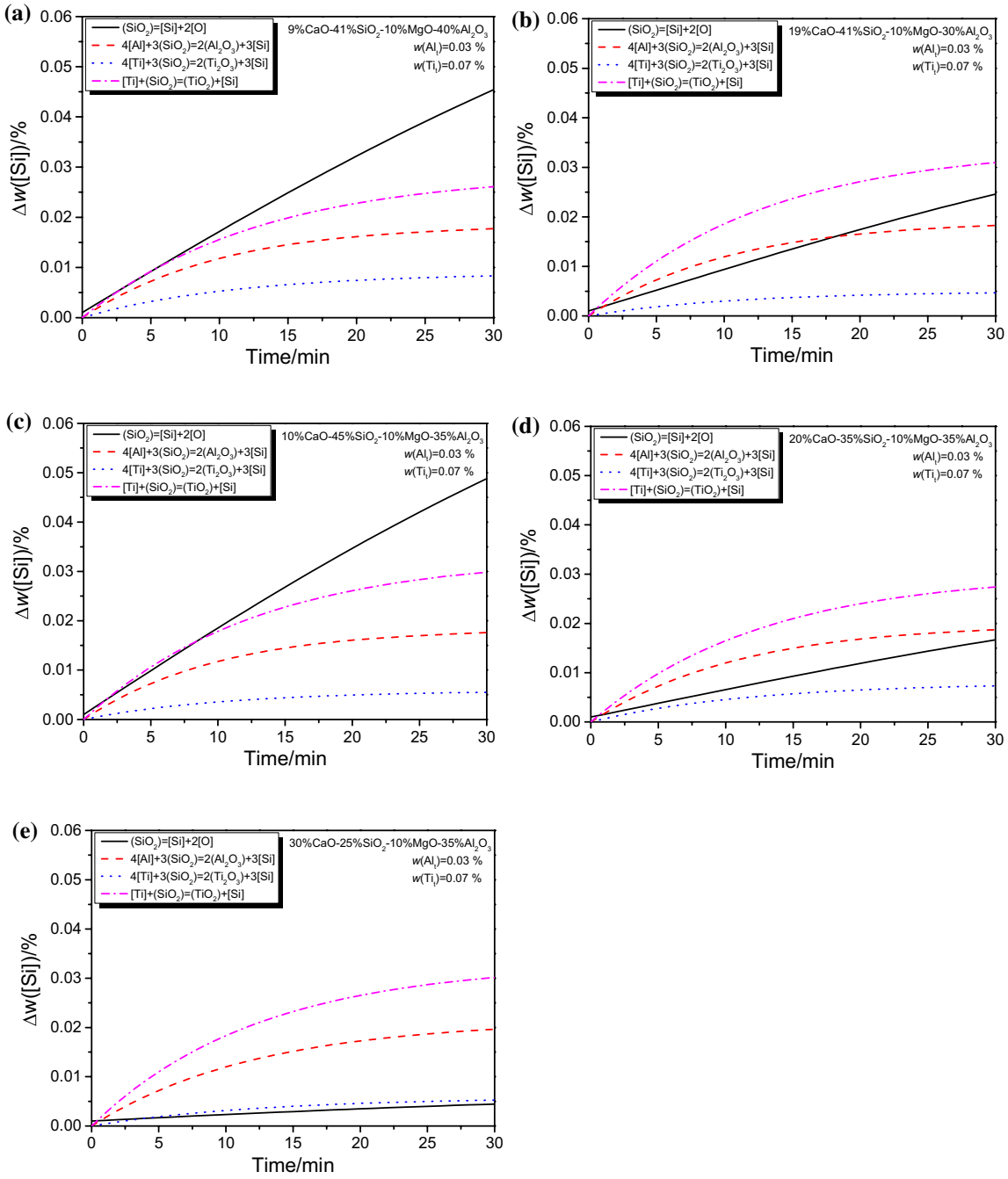

Fig. 11 Effect of initial slag chemistries on $\Delta w([Si])$ in Al–Ti-containing steels with 0.03% Al_t and 0.07% Ti_t

4.2 Effect of initial slag chemistries on reoxidation behavior

Figure 8 shows the effect of the initial slag chemistries on changes in inclusions in Al–Ti-containing steels with 0.03% Al_t and 0.07% Ti_t. With the comparison of Figs. 4c and 8, the amount of the formed inclusions was slightly reduced by increasing the ratio of CaO to Al_2O_3, while it was dramatically decreased by increasing the ratio of CaO to SiO_2 in CaO–Al_2O_3–10% MgO–41% SiO_2 slag. Meanwhile, the formed liquid Al_2O_3–TiO_x liquid oxides decreased or disappeared. Figure 9 shows the effect of the initial slag chemistries on changes in w([Al]) and w([Ti]) in Al–Ti-containing steels with 0.03% Al_t and 0.07% Ti_t. Increasing the ratios of CaO to Al_2O_3 and CaO to SiO_2 in the slag is beneficial to suppress the reoxidation of [Ti] by the slag, giving rise to the reduction of dw([Ti])/dw([Al]) during slag reoxidation process, as shown in Fig. 10.

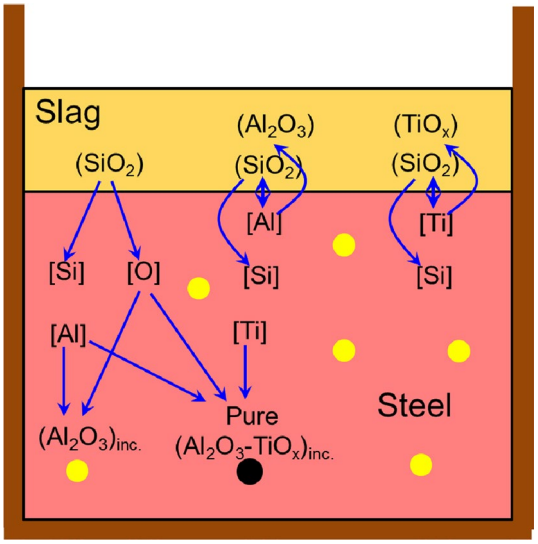

Fig. 12 Schematic diagram for reactions occurring during slag reoxidation process

Figure 11 shows the effect of the initial slag chemistries on Δw([Si]) in Al–Ti-containing steels with 0.03% Al_t and 0.07% Ti_t. As shown in Fig. 11a, the increase in the ratio of CaO to Al_2O_3 in the slag can lower the Δw([Si]) caused by the self-dissociation of SiO_2 and promote the reduction of SiO_2 in the slag by [Al]. It should be noted that increasing the ratio of CaO to SiO_2 in the slag can effectively suppress the self-dissociation of SiO_2 into [Si] and [O]. Thus, it was indicated that the self-dissociation of SiO_2 was significantly influenced by the slag composition instead of $w(Al_t)$ and $w(Ti_t)$ in the current calculation condition.

Figure 12 shows the schematic diagram for the reactions occurring during reoxidation of Al–Ti-containing steels by CaO–Al_2O_3–SiO_2–MgO slags. The SiO_2 in the slag was confirmed to be the only source of oxygen owing to its stronger oxidability. The [Al] and [Ti] were oxidized by the SiO_2 in the slag as Eqs. (8)–(10), which were dependent on the w([Al]), w([Ti]), and slag composition. In addition, the self-dissociation of SiO_2 in the slag occurred and produced oxygen to steel during the reoxidation process. In the current calculated cases, the initial inclusions were solid Al_2O_3. With the increase in [O] from the self-dissociation of SiO_2, the [Al] and [Ti] were reoxidized to Al_2O_3 or Al_2O_3–TiO_x inclusions, as Eqs. (1) and (2). Additionally, there was no TiO_x formed during the slag reoxidation process. Moreover, reactions between solid Al_2O_3 inclusions and [Ti] can hardly occur during reoxidation in the current simulated case.

5 Conclusions

1. A kinetic model was developed using FactSage Macro Processing to better understand the slag–steel–inclusions reactions during reoxidation of Al–Ti-containing steels by CaO–Al_2O_3–SiO_2–MgO slags. The calculated results show a good agreement with the experimental data from the literature.
2. During the slag reoxidation process, the [Al] and [Ti] were oxidized by the SiO_2 in the slag, which was dependent on the w([Al]), w([Ti]), and slag composition. In addition, the reaction of self-dissociation of SiO_2 in the slag into [Si] and [O] can be suppressed by increasing the ratios of CaO to SiO_2 and CaO to Al_2O_3 in the slag.
3. During the slag reoxidation process, the [Al] and [Ti] reacted with the [O] from the self-dissociation of SiO_2 in the slag and formed inclusions changing from solid Al_2O_3 to Al_2O_3–TiO_x inclusions. The inclusion chemistry was mainly dependent on the w([Al]) and w([Ti]), while the amount of inclusions can be reduced by increasing the ratios of CaO to SiO_2 and CaO to Al_2O_3 in the slag.

Acknowledgements The authors are grateful for support from the National Key R&D Program of China (2017YFB0304000, 2017YFB0304001), National Natural Science Foundation of China (Grant Nos. 51725402 and 51704018), the Fundamental Research Funds for the Central Universities (Grant Nos. FRF-TP-15-001C2 and FRF-TP-17-039A1), Guangxi Key Research and Development Plan (Grant No. AB17129006), National Postdoctoral Program for Innovative Talents (Grant No. BX201700028), Young Elite Scientists Sponsorship Program by CAST (No. 2017QNRC001), China Postdoctoral Science Foundation (No. 2017M620016), Beijing Key Laboratory of Green Recycling and Extraction of Metals (GREM) and the High Quality Steel Consortium (HQSC), and Green Process Metallurgy and Modeling (GPM^2) at the School of Metallurgical and Ecological Engineering at University of Science and Technology Beijing (USTB), China.

References

[1] L. Zhang, B.G. Thomas, ISIJ Int. 43 (2003) 271–291.
[2] L. Zhang, B.G. Thomas, Metall. Mater. Trans. B 37 (2006) 733–761.
[3] W. Yang, Y. Zhang, L.F. Zhang, H.J. Duan, L. Wang, J. Iron Steel Res. Int. 22 (2015) 1069–1077.
[4] D.C. Park, I.H. Jung, P.C.H. Rhee, H.G. Lee, ISIJ Int. 44 (2004) 1669–1678.
[5] Q. Zhang, L. Wang, X. Wang, ISIJ Int. 46 (2006) 1421–1426.
[6] C. Wang, N. Verma, Y. Kwon, W. Tiekink, N. Kikuchi, S. Sridhar, ISIJ Int. 51 (2011) 375–381.
[7] S. Basu, S.K. Choudhary, N.U. Girase, ISIJ Int. 44 (2004) 1653–1660.
[8] C. Bernhard, G. Xia, M. Egger, A. Pissenberger, S.K. Michelic, in: AISTech 2012, Association for Iron and Steel Technology, Pittsburg, PA, United States, 2012, pp. 2191–2200.
[9] C. Wang, N.T. Nuhfer, S. Ridhar, Metall. Mater. Trans. B 41 (2009) 1006–1021.
[10] C. Wang, N.T. Nuhfer, S. Sridhar, Metall. Mater. Trans. B 40 (2009) 1022–1034.
[11] C. Wang, N.T. Nuhfer, S. Sridhar, Metall. Mater. Trans. B 41 (2010) 1084–1094.

[12] M. Wang, Y.P. Bao, H. Cui, H.J. Wu, W.S. Wu, ISIJ Int. 50 (2010) 1606–1611.
[13] E. Zinngrebe, C.V. Hoek, H. Visser, A. Westendorp, I.H. Jung, ISIJ Int. 52 (2012) 52–61.
[14] C. Lyons, P. Kaushik, Steel Res. Int. 82 (2011) 1394–1403.
[15] W.C. Doo, D.Y. Kim, S.C. Kang, K.W. Yi, Met. Mater. Int. 13 (2007) 249–255.
[16] M.K. Sun, I.H. Jung, H.G. Lee, Met. Mater. Int. 14 (2008) 791–798.
[17] Y. Wang, S. Sridhar, A.W. Sridhar, A. Gomez, C. Cicutti, Iron Steel Technol. 1 (2004) 87–96.
[18] Y. Higuchi, Y. Tago, K. Takatani, S. Fukagawa, Tetsu-to-Hagané 84 (1998) 333–338.
[19] Y. Qin, X. Wang, L. Li, F. Huang, Steel Res. Int. 86 (2015) 1037–1045.
[20] A. Harada, N. Maruoka, H. Shibata, S.Y. Kitamura, ISIJ Int. 53 (2013) 2110–2117.
[21] A. Harada, N. Maruoka, H. Shibata, S.Y. Kitamura, ISIJ Int. 53 (2013) 2118–2125.
[22] P.R. Scheller, Q. Shu, Steel Res. Int. 85 (2014) 1310–1316.
[23] M.A. Van Ende, I.H. Jung, Metall. Mater. Trans. B 48 (2017) 28–36.
[24] S.P.T. Piva, D. Kumar, P.C. Pistorius, Metall. Mater. Trans. B 48 (2017) 37–45.
[25] J.H. Shin, Y. Chung, J.H. Park, Metall. Mater. Trans. B 48 (2017) 46–59.
[26] J. Peter, K.D. Peaslee, D.G.C. Robertson, B.G. Thomas, in: AISTech 2005, Association for Iron and Steel Technology, Charlotte, NC, 2005, pp. 959–973.
[27] Y. Ren, Y. Zhang, L. Zhang, Ironmak. Steelmak. 44 (2016) 497–504.
[28] I.H. Jung, S.A. Decterov, A.D. Pelton, ISIJ Int. 44 (2004) 527–536.
[29] D. Roy, P.C. Pistorius, R.J. Fruehan, Metall. Mater. Trans. B 44 (2013) 1086–1094.